

# Superconductivity in the pseudogap region of $\text{Bi}_2\text{Sr}_{1.4}\text{La}_{0.6}\text{CuO}_{6+\delta}$ from angular-dependent torque measurements

T. Hu,<sup>1</sup> H. Xiao,<sup>1,2</sup> P. Gyawali,<sup>1</sup> H. H. Wen,<sup>3</sup> and C. C. Almasan<sup>1</sup><sup>1</sup>*Department of Physics, Kent State University, Kent, Ohio 44242, USA*<sup>2</sup>*Beijing National Laboratory for Condensed Matter Physics, Institute of Physics, Chinese Academy of Sciences, Beijing 100190, China*<sup>3</sup>*Department of Physics, Nanjing University, Nanjing 210093, China*

(Received 12 February 2012; published 16 April 2012)

We show in-plane and out-of-plane angular dependent torque data on underdoped  $\text{Bi}_2\text{Sr}_{1.4}\text{La}_{0.6}\text{CuO}_{6+\delta}$  single crystals. We find that the superconducting signal persists well into the normal state, at least up to twice the zero-field superconducting transition temperature  $T_{c0}$ . The superconductivity is highly anisotropic below  $T_{c0}$ , while its anisotropy decreases significantly just above  $T_{c0}$ . In this latter  $T$  regime the Cooper pairs lose their long-range phase coherence.

DOI: [10.1103/PhysRevB.85.134516](https://doi.org/10.1103/PhysRevB.85.134516)

PACS number(s): 74.20.Rp, 74.25.Ha, 74.72.Gh, 74.72.Kf

## I. INTRODUCTION

The mechanism of high transition temperature superconductivity in cuprates is not fully understood after more than twenty years from their discovery. The origin of the pseudogap and its relationship to the superconducting gap are believed to hold the key to the understanding of this mechanism. However, it is still an issue of intense debate whether the pseudogap and superconducting gap have same origin, or whether they are two competing order phases.<sup>1</sup>

On one hand, it is thought that the pseudogap phase is a precursor of some hidden ordered state and that its fluctuations are responsible for the pairing of cuprates,<sup>2</sup> which makes the cuprates similar to the heavy fermion, organic, and iron based superconductors. NMR measurements on  $\text{Bi}_2\text{Sr}_{1-x}\text{La}_x\text{CuO}_{6+\delta}$  (Ref. 3) and angle-resolved photoemission spectroscopy measurements on  $\text{Bi}_2\text{Sr}_2\text{Ca}_{1-x}\text{Y}_x\text{Cu}_2\text{O}_8$  (Ref. 4) have suggested that the pseudogap and superconducting gap are two coexisting matters.

On the other hand, there is growing evidence for the presence of vortices in the pseudogap region of underdoped cuprate superconductors, indicating that the superconducting gap survives above the zero-field superconducting transition temperature  $T_{c0}$  while phase fluctuations in the pseudogap state destroy the long-range phase coherence of the Cooper pairs. For example, high-frequency conductivity measurements on underdoped  $\text{Bi}_2\text{Sr}_2\text{CaCu}_2\text{O}_{8+\delta}$  (Ref. 5) and angular magnetoresistivity measurements on underdoped  $\text{Y}_{1-x}\text{Pr}_x\text{Ba}_2\text{Cu}_3\text{O}_{7-\delta}$  (Refs. 6 and 7) have shown that the motion of vortices persists above the zero-field superconducting transition temperature  $T_{c0}$ . Vortexlike excitations and the onset of superconducting phase fluctuations at temperatures as high as 150 K were observed in underdoped  $\text{La}_{2-x}\text{Sr}_x\text{CuO}_4$  by Nernst effect measurements.<sup>8</sup> Magnetic imaging of  $\text{La}_{2-x}\text{Sr}_x\text{CuO}_4$  thin films has revealed inhomogeneous magnetic domains that persist up to 80 K, while  $T_{c0}$  of the films is only  $\sim 18$  K, suggesting the existence of diamagnetic regions that are precursors to the Meissner state.<sup>9</sup> A field enhanced diamagnetic signal, which is associated with the existence of superconductivity, is observed in  $\text{Bi}_2\text{Sr}_2\text{CaCu}_2\text{O}_{8+\delta}$  above  $T_{c0}$  (Ref. 10). Specific heat measurements reveal evidence of residual superconductivity in underdoped  $\text{Bi}_2\text{Sr}_{2-x}\text{La}_x\text{CuO}_{6+\delta}$  far above  $T_{c0}$  (Ref. 11). Very recent high field (up to 45 T) specific heat measurements

on  $\text{YBa}_2\text{Cu}_3\text{O}_{6.56}$  show that the magnetic field  $H$  dependence of the quasiparticle density of states follows an  $\sqrt{H}$  behavior that persists smoothly through  $T_{c0}$ , well into the magnetic field induced resistive state.<sup>12</sup>

In contrast to transport measurements, such as conductivity and the Nernst effect, torque is both a thermodynamic and a bulk measurement. It is a sensitive tool to probe the symmetry of the superconducting energy gap and the anisotropy of superconductivity. This motivated us to perform angular dependent torque measurements of underdoped  $\text{Bi}_2\text{Sr}_{1.4}\text{La}_{0.6}\text{CuO}_{6+\delta}$  single crystals both below and above  $T_{c0}$  in order to obtain further insight into the nature of superconductivity and vortex matter in the pseudogap region. Our out-of-plane torque data show that a diamagnetic signal persists into the normal state up to about 50 K, a temperature twice as high as  $T_{c0} = 25$  K, while the pseudogap temperature is much higher, i.e., 200 K. These data also show that the anisotropy  $\gamma$  of this system is strongly temperature  $T$  dependent, with large values ( $\gamma \sim 100$ ) at low temperatures, confirming the two-dimensional (2D) nature of superconductivity in this system below  $T_{c0}$ , and small values ( $\gamma \sim 1$ ) just above  $T_{c0}$ , indicating that superconductivity becomes weakly anisotropic in this latter  $T$  range;  $\gamma \equiv \sqrt{m_c^*/m_a^*}$ , where  $m_c^*$  and  $m_a^*$  are the effective masses along the  $c$  and  $a$  crystallographic directions, respectively. Our in-plane torque measurements confirm that the Cooper pairs lose their long-range phase coherence above  $T_{c0}$ . These results could suggest that the Cooper pairs are localized above  $T_{c0}$  in small regions of the single crystal that is consistent with the scenario of competing orders between the pseudogap and superconducting phases.

## II. EXPERIMENTAL DETAILS

Single crystals of underdoped  $\text{Bi}_2\text{Sr}_{1.4}\text{La}_{0.6}\text{CuO}_{6+\delta}$  were grown using the traveling-solvent floating-zone technique.<sup>13</sup> The zero-field superconducting transition temperature  $T_{c0} = 25$  K for the crystal for which data are reported here. We determined this value from the  $T$ -dependent magnetization  $M$  measurement done in a 10 Oe applied magnetic field  $H$  (see open symbols in Fig. 1). The in-plane and out-of-plane angular-dependent torque was measured over a wide range of temperatures and in applied magnetic fields up to 14 T by using a piezoresistive torque magnetometer. The contributions of the

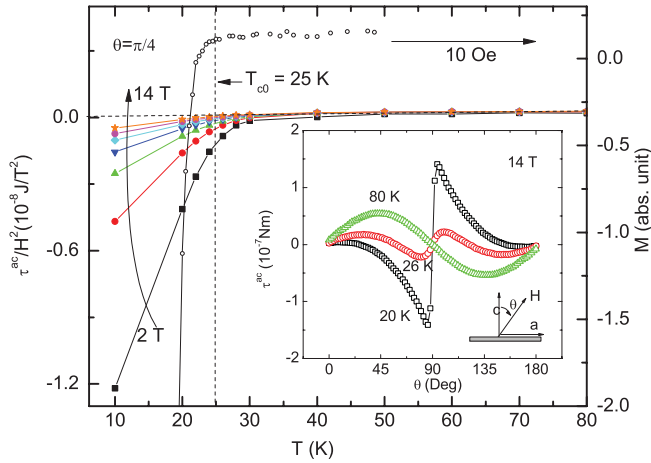


FIG. 1. (Color online) Temperature  $T$  dependence of  $\tau^{ac}/H^2$  ( $\tau^{ac}$  is the out-of-plane torque), measured in an applied magnetic field  $H = 2, 4, 6, 8, 10, 12, 14$  T, and of magnetization  $M$  measured at 10 Oe on a  $\text{Bi}_2\text{Sr}_{1.4}\text{La}_{0.6}\text{CuO}_{6+\delta}$  single crystal. Inset: Angular  $\theta$  dependent  $\tau^{ac}$  measured at 20, 26, and 80 K and 14 T.

gravity and puck to the total torque signal were measured and subtracted from it as discussed elsewhere.<sup>14</sup> The angles  $\theta$  and  $\varphi$  are the angles between  $H$  and the crystallographic  $c$  axis (inset to Fig. 1) and  $a$  axis [inset to Fig. 4(a)], respectively, of the single crystal.

### III. RESULTS AND DISCUSSION

#### A. Out-of-plane torque measurements

We show in the inset to Fig. 1 angular  $\theta$  dependent out-of-plane reversible torque  $\tau^{ac}$  data measured in 14 T and at 20, 26, and 80 K. The 80 K data show the typical angular dependence of the paramagnetic torque  $\tau_p^{ac}(\theta)$ , with the amplitude reflecting the anisotropy between the susceptibilities  $\chi_c$  and  $\chi_a$ , along the  $c$  and  $a$  axes, respectively, since

$$\tau_p^{ac}(\theta) \equiv \frac{\chi_c - \chi_a}{2} H^2 \sin 2\theta. \quad (1)$$

As shown later, the 26 K data incorporate both  $\tau_p^{ac}(\theta)$  and the torque signal  $\tau_{sc}^{ac}(\theta)$  due to superconductivity. This latter torque signal is given by the Abrikosov vortex matter in an anisotropic superconductor;<sup>15,16</sup> hence it reflects the presence of vortices and the anisotropy of superconductivity. The angular dependence of the 20 K torque is typical of  $\tau_{sc}^{ac}(\theta)$ , implying that the paramagnetic signal is negligible at this temperature (i.e.,  $\tau_p^{ac} \ll \tau_{sc}^{ac}$ ).

In order to reveal the paramagnetic and diamagnetic contributions to the measured torque and to be able to separate these contributions, we plot in Fig. 1 the  $T$  dependence of reversible  $\tau^{ac}/H^2$  (solid symbols), measured at  $\theta = 45^\circ$  [for which  $\sin(2\theta) = 1$  in Eq. (1)] and in fields up to 14 T. Notice that  $\tau^{ac}/H^2$  is negative and its magnitude decreases with increasing  $H$  for low temperatures, which is typical of the torque signal due to superconductivity. At higher temperatures,  $\tau^{ac}/H^2$  becomes positive and the data overlap for different  $H$  values. This higher temperature regime corresponds to a pure paramagnetic state, with only paramagnetic torque  $\tau_p^{ac}$  present.

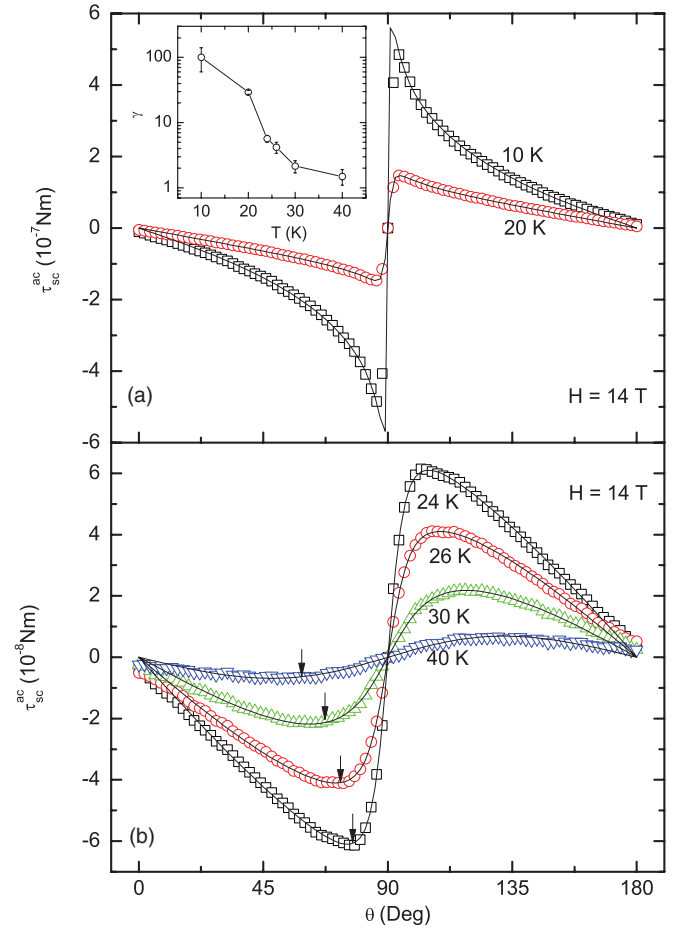


FIG. 2. (Color online) Angular  $\theta$  dependent torque due to superconductivity  $\tau_{sc}^{ac}$ , measured at 14 T and at temperatures (a)  $T < T_{c0}$  (10, 20 K) and (b)  $T > T_{c0}$  (24, 26, 30, 40 K). Inset to (a):  $T$  dependence of anisotropy parameter  $\gamma$ .

The dashed line shows the  $T$  dependence of  $(\chi_c - \chi_a)/2$  in this pure paramagnetic state [see Eq. (1)], while its extrapolation to lower temperatures facilitates the determination of the paramagnetic torque at these temperatures. Also notice that the temperatures at which the pure paramagnetic region sets in are much higher than  $T_{c0}$ .

We plot in Figs. 2(a) and 2(b)  $\tau_{sc}^{ac}(\theta)$  that we obtained from the torque data measured at 14 T and temperatures below and above  $T_{c0}$ , respectively, after subtracting the paramagnetic torque determined as just discussed. Notice that the 10 and 20 K torque signals first increase in magnitude with increasing angle, they display a sharp peak for  $\theta$  very close to  $90^\circ$ , and then they are symmetric with respect to zero, reversing sign for  $\theta$  just above  $90^\circ$ . This is a typical behavior of the torque in the mixed state of an extremely anisotropic, hence a 2D superconductor, with a large anisotropy parameter  $\gamma$ ; the supercurrents are confined in this case to the  $ab$  plane of the crystal and the magnetic moment produced by these supercurrents can only be parallel or antiparallel with the  $c$  axis of the crystal, giving rise to the jump and sign reversal in the torque signal when the applied magnetic field is in the  $ab$  plane, i.e., it makes an angle of  $90^\circ$  with the  $c$  axis.<sup>17</sup>

In less anisotropic superconductors, the change in sign in  $\tau_{sc}^{ac}(\theta)$  produces a more rounded peak which is at  $\theta < 90^\circ$  (Ref. 17). Notice that this is the case for our torque curves measured at  $T > T_{c0}$  [Fig. 2(b)], with the peak becoming broader and its position (indicated by the arrow) shifting toward  $45^\circ$  as the temperature increases; overall, the shape of these curves changes toward a  $\sin 2\theta$  dependence. We discuss the reason for this evolution in the angular dependence of these torque data below. In conclusion, the similar overall behavior of the torque data of Figs. 2(a) and 2(b) indicates that vortices are also present above  $T_{c0}$ , while the evolution of the shape of these curves with increasing temperature shows a substantial decrease in the anisotropy of superconductivity at and above  $T_{c0}$ .

We were able to obtain the specific values of the anisotropy at different temperatures by fitting the torque data with the following expression for the torque of an anisotropic superconductor:<sup>15</sup>

$$\tau_{sc}^{ac}(\theta) = \frac{\phi_0 H V}{16\pi\mu_0\lambda^2} \frac{\gamma^2 - 1}{\gamma} \frac{\sin 2\theta}{\epsilon(\theta)} \ln \left\{ \frac{\gamma\eta H_{c2}}{H\epsilon(\theta)} \right\}, \quad (2)$$

where  $V$  is the volume of the sample,  $\mu_0$  is the vacuum permeability,  $\lambda$  is the in-plane penetration depth,  $\epsilon(\theta) = (\sin^2\theta + \gamma^2 \cos^2\theta)^{1/2}$ ,  $\eta$  is a numerical parameter of order unity, and  $H_{c2}$  is the upper critical field along the  $c$  axis. Such fits of the torque data of Fig. 2(a) give very large values for  $\gamma$  ( $\gamma \approx 100 \pm 40$  at 10 K and  $30 \pm 2$  at 20 K), while fits of the data of Fig. 2(b) give values of  $\gamma$  that are substantially smaller [see inset to Fig. 2(a)]. The large  $\gamma$  values measured in the mixed state are consistent with previous torque measurements on  $\text{Bi}_2\text{Sr}_{2-x}\text{La}_x\text{CuO}_{6+\delta}$  single crystals<sup>18</sup> and show that the superconductivity and vortex matter below  $T_{c0} = 25$  K are, indeed, 2D, while the small values of  $\gamma$  above  $T_{c0}$  point toward a much smaller anisotropy of superconductivity and vortex matter. Equation (2) shows that  $\tau_{sc}^{ac} \propto \sin 2\theta$  for  $\gamma \sim 1$ . This explains why the shape of the torque curves approaches  $\sin 2\theta$  as the temperature increases above  $T_{c0}$  where  $\gamma$  approaches 1.

The consistency of the above analysis of the torque data of Figs. 2(a) and 2(b) with Kogan's model<sup>15</sup> and especially the excellent fit of the data of Fig. 2(b) (measured above  $T_{c0}$ ) with this model, despite the fact that it is meant to describe the behavior of the torque for the actual  $H_{c2}$  for this system. In fact, for optimally doped  $\text{Bi}_2\text{Sr}_2\text{CaCu}_2\text{O}_{8+\delta}$ , which also shows the presence of vortices above  $T_{c0}$ , the estimated  $H_{c2}$  is 200 T at 35 K and 90 T (instead of going to zero) at  $T_{c0} = 86$  K (Ref. 10).

Anisotropic or spatially textured electronic states are present in unconventional superconductors as a result of competing interactions or competing orders, which lead to textured superconductivity above the bulk superconducting transition temperature  $T_{c0}$  (Ref. 19). Therefore, in the case of a 2D normal-state electronic structure, as reported for the underdoped  $(\text{Bi,Pb})_2(\text{Sr,L a})_2\text{CuO}_{6+\delta}$  samples,<sup>20</sup> one expects an anisotropic superconductivity at least just above  $T_{c0}$  or even at higher temperatures. However, this is not the case based on the present experimental results of the  $\gamma$  values. This leads us to speculate that, due to competing pseudogap and superconducting orders,<sup>4</sup> superconductivity above  $T_{c0}$

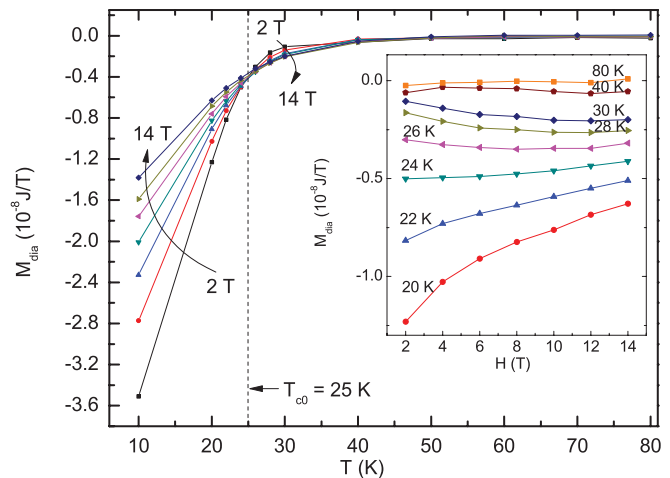


FIG. 3. (Color online) Temperature  $T$  dependence of diamagnetic magnetization  $M_{\text{dia}}$  [ $M_{\text{dia}} \equiv \tau_{sc}^{ac}/[H \sin(\pi/4)]$ ] measured in a magnetic field  $H = 2, 4, 6, 8, 10, 12, 14$  T. The dashed line shows the zero-field superconducting transition temperature  $T_{c0}$ . Inset:  $H$  dependent  $M_{\text{dia}}$  measured from 20 to 80 K.

“survives” in regions where the pseudogap order is locally suppressed. This gives rise to small superconducting islands above  $T_{c0}$  in the pseudogap region, with an incoherent state for both the  $ab$  plane and  $c$  axis, hence with an anisotropy  $\gamma$  approaching 1.

We show in Fig. 3 the  $T$ -dependent diamagnetic magnetization  $M_{\text{dia}} \equiv \tau_{sc}^{ac}(\pi/4)/[H \sin(\pi/4)]$ , obtained from the measured reversible torque  $\tau^{ac}(\pi/4)$  after subtracting the paramagnetic torque. We note that  $M_{\text{dia}} \equiv \tau_{sc}^{ac}/[H \sin(\pi/4)] = M_c - M_{ab}$  ( $M_c$  and  $M_{ab}$  are the  $c$  and  $ab$  components, respectively, of the diamagnetic magnetization) since  $\tau_{sc}^{ac}(\theta) \equiv \vec{M} \times \vec{H} = M_c H \sin\theta - M_{ab} H \cos\theta$ . For highly anisotropic superconductors ( $\gamma \gg 1$ ),  $|M_c|$  is much larger than  $|M_{ab}|$ ; therefore  $M_{\text{dia}}$  reflects the diamagnetic signal of superconductivity in the  $c$  direction, while for a superconductor with small anisotropy ( $\gamma \sim 1$ ), the contribution of  $M_{ab}$  is not negligible, so  $M_{\text{dia}} = M_c - M_{ab}$ . Generally,  $|M_c| > |M_{ab}|$ ; therefore,  $M_{\text{dia}}$  is negative. Hence, a negative  $M_{\text{dia}}$  extracted from torque measurements is evidence of the presence of superconductivity. The fact that a negative  $M_{\text{dia}}$  persists up to a temperature  $T \approx 50$  K  $= 2T_{c0}$  shows that superconductivity persists to temperatures well above  $T_{c0}$ .

Furthermore, the  $H$  dependence of  $M_{\text{dia}}$  changes exactly at  $T_{c0}$  (see the main panel and the inset to Fig. 3). Specifically, the magnetic field suppresses the diamagnetic signal below  $T_{c0}$ , while it enhances the diamagnetism above  $T_{c0}$ . This field-enhanced diamagnetism is similar to a previous report on underdoped  $\text{Bi}_2\text{Sr}_2\text{Ca}_2\text{CuO}_{8+\delta}$  (Ref. 10). It has been shown theoretically that such an abnormal field-dependent magnetization is due to the contribution of thermal distortions of vortices to the free energy.<sup>21</sup> Nevertheless, this theoretical work does not take into account that the anisotropy of superconductivity decreases significantly above  $T_{c0}$ . Therefore, this change of  $M_{\text{dia}}(H)$  behavior at  $T_{c0}$  could also be a result of the dimensional change of superconductivity at  $T_{c0}$ . Below  $T_{c0}$  the superconductivity is 2D-like so  $M_{\text{dia}} \approx M_c$  and

it is suppressed by an applied magnetic field. Above  $T_{c0}$ , superconductivity is much less anisotropic,  $M_{ab}$  cannot be neglected, so  $M_{\text{dia}} = M_c - M_{ab}$ , and hence it could lead to a different field-dependent behavior.

### B. In-plane torque measurements

Until now we have shown through out-of-plane torque data measured on  $\text{Bi}_2\text{Sr}_{1.4}\text{La}_{0.6}\text{CuO}_{6+\delta}$  that superconductivity and vortices persist into the normal state inside the pseudogap region, which extends up to about 200 K for this particular doping level.<sup>3</sup> We next determine if there is a long-range phase coherence between the Cooper pairs above  $T_{c0}$  through in-plane torque measurements. These measurements were previously successfully used to probe the symmetry of the superconducting gap,<sup>14,22,23</sup> thus giving the phase correlation between the Cooper pairs. Torque is a bulk measurement so it provides information on the order parameter of the bulk, not only the surface. It also *directly* probes the nodal positions on the Fermi surface with high angular resolution since torque is the angular derivative of the free energy ( $F$ ), i.e.,  $\tau(\varphi) = -\partial F(\varphi)/\partial\varphi$ .

We plot in Fig. 4(a) and the inset to Fig. 4(a) the angular  $\varphi$  dependent torque data measured in different applied magnetic fields up to 14 T at temperatures of 15 to 20 K and for 25 K (at  $T_{c0}$ ), respectively. The amplitude of the torque signal decreases as the temperature approaches  $T_{c0}$  and eventually the signal is scattered around zero for  $T \geq T_{c0}$ . The solid line in Fig. 4(a) is a fit of the torque data measured at 15 K and 14 T with  $\tau^{ab} = \tau_2 \sin 2(\varphi - m_2) + \tau_4 \sin 4(\varphi - m_4)$ , where  $\tau_2$ ,  $\tau_4$ ,  $m_2$ , and  $m_4$  are the four fitting parameters. Notice that the fitting curve follows the general trend of the data, but clearly there are other terms missing from this fitting expression.

We show in Figs. 4(b) and 4(c) the magnetic field dependence of these four fitting parameters extracted by fitting the in-plane torque data measured at 15 K and in magnetic fields up to 14 T. Notice that both  $\tau_2$  and  $\tau_4$  increase with increasing  $H$  up to 14 T. A small misalignment between the magnetic field and the  $ab$  plane of the single crystal could give a two-fold symmetry term, i.e., a  $\sin 2(\varphi - \varphi_0)$  term.<sup>24</sup> However, Fig. 4(c) shows that both  $m_2$  and  $m_4$  increase with increasing  $H$ , but their difference  $\Delta m = m_4 - m_2 \approx 45^\circ$  over the whole measured field range. This lock-in phase of  $m_2$  and  $m_4$  suggests that both the two-fold and four-fold symmetries are intrinsic, are due to superconductivity, and have the same nature, excluding the misalignment scenario for the two-fold symmetry term.

The four-fold symmetry of the torque measured in the superconducting state reflects the gap symmetry, which is determined by the direction of the diamagnetic magnetization  $M$  (Refs. 14,22, and 23). Since  $\varphi$  gives the direction of  $H$  and since  $M$  and  $H$  are in opposite directions *only* for large  $H$  values, only parameters  $m_4$  of the four-fold symmetry extracted by fitting in-plane torque data measured in high  $H$  give the correct nodal positions of the superconducting gap. Notice from Fig. 4(c) that  $m_4$  approaches  $45^\circ$  while  $m_2$  approaches zero at large  $H$  values, which gives  $\tau^{ab} = \tau_2 \sin 2\varphi - \tau_4 \sin 4\varphi$ . This four-fold symmetry of the torque corresponds to the  $d_{x^2-y^2}$  wave symmetry of the superconducting gap, which

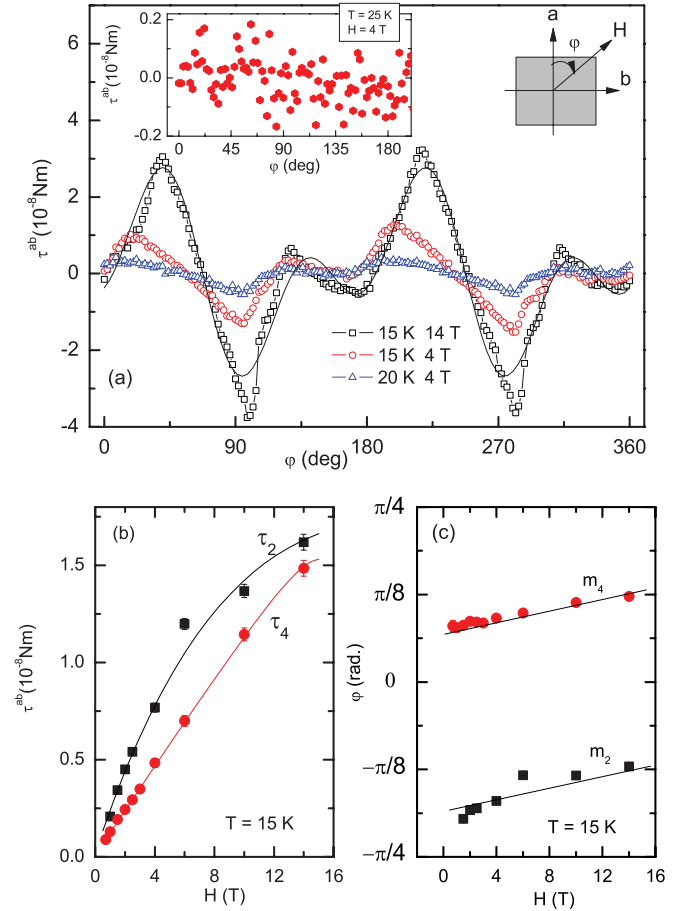


FIG. 4. (Color online) (a) In-plane angular dependent torque  $\tau^{ab}$  measured at a temperatures  $T = 15, 20, 25$  K and in an applied magnetic field of 4 and 14 T. The solid line is a fit of the data with  $\tau^{ab} = \tau_2 \sin 2(\varphi - m_2) + \tau_4 \sin 4(\varphi - m_4)$ . Right inset: Magnetic field  $H$  is rotated in the  $ab$  plane and makes an angle  $\varphi$  with the  $a$  crystallographic direction. Left inset:  $\tau^{ab}$  measured at  $T = T_{c0} = 25$  K and 4 T. (b) and (c) are the field  $H$  dependent  $\tau_2$  and  $\tau_4$ , and  $m_2$  and  $m_4$ , respectively.

is already agreed upon for cuprates, since it has a  $-\sin 4\varphi$  angular dependence.<sup>14</sup> Furthermore, it reflects the existence of a long-range phase coherence between the Cooper pairs in this system. The zero amplitude of the in-plane torque above  $T_{c0}$  shows that the Cooper pairs lose their long-range phase coherence at these temperatures.

There are two possibilities for the additional two-fold symmetry of the in-plane torque below  $T_{c0}$ , which we believe is intrinsic. One possibility is that an  $s$  wave symmetry is present in the mixed state of this system, besides the  $d_{x^2-y^2}$  wave symmetry. Another possibility is that it reflects the broken four-fold rotation symmetry (due to stripe or nematic order) associated with the pseudogap phase.<sup>2,25</sup>

### IV. CONCLUSIONS

In summary, superconductivity persisting up to temperatures as high as twice the zero-field superconducting transition temperature  $T_{c0}$  is observed in underdoped  $\text{Bi}_2\text{Sr}_{1.4}\text{La}_{0.6}\text{CuO}_{6+\delta}$  single crystals through out-of-plane

torque measurements. Below  $T_{c0}$  the superconductivity is 2D-like and there is long-range phase coherence between the Cooper pairs. Above  $T_{c0}$ , the superconductivity has a much smaller anisotropy, which could be due to the fact that the Cooper pairs are localized in small regions, and they lose their long-range phase coherence. Our findings show that superconductivity above and below  $T_{c0}$  is of a different nature. Our results are consistent with the scenario of competing orders between the pseudogap and superconducting phases.

### ACKNOWLEDGMENTS

This research was supported at KSU by the National Science Foundation under Grants No. DMR-1006606 and No. DMR-0844115, and by ICAM Branches Cost Sharing Fund from the Institute for Complex Adaptive Matter. H.X. was supported by NSFC (Project No. 11104335) and the MOST (Project No. 2011CBA00107) and H.H.W. by NSFC and MOST (Project No. 2011CBA00102).

- 
- <sup>1</sup>A. J. Millis, *Science* **314**, 1888 (2006) .  
<sup>2</sup>L. Taillefer, *Annu. Rev. Condens. Matter Phys.* **1**, 51 (2010) .  
<sup>3</sup>Guo-qing Zheng, P. L. Kuhns, A. P. Reyes, B. Liang, and C. T. Lin, *Phys. Rev. Lett.* **94**, 047006 (2005).  
<sup>4</sup>K. Tanaka, W. S. Lee, D. H. Lu, A. Fujimori, T. Fujii, Risdiana, I. Terasaki, D. J. Scalapino, T. P. Devereaux, Z. Hussain, and Z.-X. Shen, *Science* **314**, 1910 (2006).  
<sup>5</sup>J. Corson, R. Mallozzi, J. Orenstein, J. N. Eckstein, and I. Bozovic, *Nature (London)* **398**, 221 (1999) .  
<sup>6</sup>V. Sandu, E. Cimpoeasu, T. Katuwal, Shi Li, M. B. Maple, and C. C. Almasan, *Phys. Rev. Lett.* **93**, 177005 (2004).  
<sup>7</sup>T. Katuwal, V. Sandu, C. C. Almasan, B. J. Taylor, and M. B. Maple, *Phys. Rev. B* **72**, 174501 (2005).  
<sup>8</sup>Z. A. Xu, N. P. Ong, Y. Wang, T. Kakeshita, and S. Uchida, *Nature (London)* **406**, 486 (2000) .  
<sup>9</sup>L. Lguchi, T. Yamaguchi, and A. Sugimoto, *Nature (London)* **412**, 420 (2001) .  
<sup>10</sup>Y. Wang, L. Li, M. J. Naughton, G. D. Gu, S. Uchida, and N. P. Ong, *Phys. Rev. Lett.* **95**, 247002 (2005) .  
<sup>11</sup>H.-H. Wen, G. Mu, H. Luo, H. Yang, L. Shan, C. Ren, P. Cheng, J. Yan, and L. Fang, *Phys. Rev. Lett.* **103**, 067002 (2009) .  
<sup>12</sup>S. C. Riggs, O. Vafek, J. B. Kemper, J. B. Betts, A. Migliori, F. F. Balakirev, W. N. Hardy, R. Liang, D. A. Bonn, and G. S. Boebinger, *Nat. Phys.* **7**, 332 (2011) .  
<sup>13</sup>H. Luo, P. Cheng, L. Fang, and H.-H. Wen, *Supercond. Sci. Technol.* **21**, 125024 (2008) .  
<sup>14</sup>H. Xiao, T. Hu, C. C. Almasan, T. A. Sayles, and M. B. Maple, *Phys. Rev. B* **78**, 014510 (2008) .  
<sup>15</sup>V. G. Kogan, *Phys. Rev. B* **38**, 7049 (1988) .  
<sup>16</sup>D. E. Farrell, C. M. Williams, S. A. Wolf, N. P. Bansal, and V. G. Kogan, *Phys. Rev. Lett.* **61**, 2805 (1988).  
<sup>17</sup>C. Bergemann, A. W. Tyler, A. P. Mackenzie, J. R. Cooper, S. R. Julian, and D. E. Farrell, *Phys. Rev. B* **57**, 14387 (1998) .  
<sup>18</sup>S. Kawamata, K. Okuda, T. Sasaki, and R. Yoshizaki, *J. Low Temp. Phys.* **117**, 891 (1999) .  
<sup>19</sup>S. A. Kivelson, E. Fradkin, and V. J. Emery, *Nature (London)* **393**, 550 (1998) .  
<sup>20</sup>T. Takeuchi, T. Kondo, T. Kitao, H. Kaga, H. Yang, H. Ding, A. Kaminski, and J. C. Campuzano, *Phys. Rev. Lett.* **95**, 227004 (2005).  
<sup>21</sup>L. N. Bulaevskii, M. Ledvij, and V. G. Kogan, *Phys. Rev. Lett.* **68**, 3773 (1992).  
<sup>22</sup>T. Ishida, K. Okuda, H. Asaoka, Y. Kazumata, K. Noda, and H. Takei, *Phys. Rev. B* **56**, 11897 (1997) .  
<sup>23</sup>M. Willemin, C. Rossel, J. Hofer, H. Keller, Z. F. Ren, and J. H. Wang, *Phys. Rev. B* **57**, 6137 (1998) .  
<sup>24</sup>I. Aviani, M. Miljak, V. Zlatić, K. D. Schotte, C. Geibel, and F. Steglich, *Phys. Rev. B* **64**, 184438 (2001) .  
<sup>25</sup>R. Daou, J. Chang, David LeBoeuf, Olivier Cyr-Choinie, Francis Laliberte, Nicolas Doiron-Leyraud, B. J. Ramshaw, Ruixing Liang, D. A. Bonn, W. N. Hardy, and Louis Taillefer, *Nature (London)* **463**, 519 (2010).